N 70 24348
NASA CR 109398

DEFORMATION PROCESSES IN FORGING CERAMICS

Progress Report No. 2

19 September - 19 December 1969

Prepared for

Office of Advanced Research and Technology
National Aeronautics and Space Administration
Headquarters
Washington, D.C.

Contract NASW-1914

by

R.M. Cannon
W.H. Rhodes

CASE FILE
COPY

AVCO CORPORATION
Systems Division
Lowell Industrial Park
Lowell, Massachusetts 01851

DEFORMATION PROCESSES IN FORGING CERAMICS

Progress Report No. 2

19 September - 19 December 1969

Prepared for

Office of Advanced Research and Technology
National Aeronautics and Space Administration
Headquarters
Washington, D.C.

Contract NASW-1914

by

R.M. Cannon
W.H. Rhodes

Approved by

T. Vasilos
T. Vasilos

AVCO CORPORATION
Systems Division
Lowell Industrial Park
Lowell, Massachusetts 01851

ABSTRACT

The program objective is to investigate the deformation processes involved in the forging of refractory ceramic oxides. Mechanical testing involving investigation of both flow and fracture processes are presently underway.

Preliminary results of a series of multiple loading, bend tests on fine-grained alumina are reported here. The mechanical results show strong strain hardening effects and an apparent Bauschinger effect. The fracture condition is suggested to depend heavily upon attaining a critical stress; some increase in the fracture stress is indicated as a result of prior strain at lower stresses.

Microstructural examination of tested specimens revealed extensive evidence for grain boundary sliding. The compressive surfaces revealed more deformation features than the tensile surfaces; some of these features are suggestive of dislocation motion. Evidence of strain enhanced grain growth was presented; this may be responsible for some of the apparent strain hardening.

FOREWORD

This work is being performed under the sponsorship of the NASA Headquarters, Office of Advanced Research and Technology, Research Division with Mr. J. Gangler as Project Monitor under Contract NASW-1914.

The work is being performed at the Avco Corporation, Systems Division, Lowell, Massachusetts in the Materials Sciences Department under the direction of Dr. T. Vasilos. R.M. Cannon is in charge of the work and is being assisted by Dr. W.H. Rhodes. The authors wish to acknowledge the assistance of B. MacAllister in Mechanical Testing and the microscopy of P.L Burnett and C.L. Houck.

TABLE OF CONTENTS

ABSTRACT

FOREWORD

I. INTRODUCTION 1

II. MECHANICAL TEST RESULTS. 1

III. MICROSTRUCTURAL EXAMINATION. 6

IV. DISCUSSION 10

V. FUTURE WORK. 16

VI. REFERENCES 16

LIST OF ILLUSTRATIONS

Figure No.		
1	Apparent Stress vs. Strain Curve for Specimen FLUX-31 Tested at 1450°C and $\dot{\varepsilon} = 1.1 \times 10^{-4} sec^{-1}$ . .	3
2	Apparent Stress vs. Strain Curve for Specimen FLUX-33 Tested at 1450°C.	4
3	Specimen FLUX-33 After Testing Showing the Non-uniform Strain Caused by More Rapid Hardening of the Gage Section	7
4	Crack in Specimen FLUX-33. This developed during the 5th cycle (a) and enlarged slightly after the 7th cycle (b)	8
5	Surface Replicas Showing Distorted Boundaries and Triple Grain Junctions.	9
6	Compressive and Tensile Surfaces after the 1st and 2nd Cycles, Respectively, for Specimen FLUX-33.	11
7	Compressive and Tensile Surfaces after the 6th Cycle for Specimen FLUX-33.	12
8	Fine Surface Steps Seen Primarily on Compression Surfaces which are Suggestive of Fine Slip Bands. . . .	13
9	Polished and Etched Cross-Sections from Specimen FLUX-30 Showing Distorted Boundaries and Triple Junctions	14

TABLE

Table No.		
I	Grain Growth in Successive Test Cycles at 1450°C . . .	15

I. INTRODUCTION

The objective of this program is to investigate the forgability of the refractory oxides. The approach taken includes an investigation of the high temperature yielding and fracture behavior of these materials in order to provide information and understanding which can them be applied directly to forging problems. In the first part of the program emphasis has been on mechanical properties studies. Forging experiments will be conducted later in the program and correlated with these results.

The first progress report, included reviews of the work and understanding to date of the high temperature mechanical behavior of the oxides as well as hot working efforts with these materials.[1] On the basis of this study, two systems were identified for primary investigation. These were fine-grained Al_2O_3, doped to exhibit grain growth, and MgO which will probably require temperatures in excess of 2100°C in order to obtain sufficient tensile ductility. Spinel ($MgAl_2O_4$) was tentatively selected for later investigation.

Some preliminary mechanical test results on 1-2 μ Al_2O_3 were also reported in the last report.[1] These studies were continued during this period and are reported here. Multiple loading in flexure was done in order to investigate the effects of multiple step deformation, intermediate annealing and reversed loading on the mechanical behavior. These various effects are particularly relevant to forging and also provide insight into fundamental mechanical processes and mechanisms. The investigation has included extensive microstructural as well as mechanical observations.

II. MECHANICAL TEST RESULTS

A series of multiple loading, bend tests on fine-grained Al_2O_3 is in progress and the results are being analyzed. The test procedure involves bending a specimen in four-point loading to a selected strain and then reversing the bar and bending it back again. The process is then repeated so the bar is bent through the range of $-\epsilon_o$ to $+\epsilon_o$ on each cycle. The maximum strain value allowed by the apparatus is 4 to 5% depending upon specimen size. The tests to date have been done primarily at 1450°C over a range of strain rates. The effects of unloading and of holding at temperature for various times are also being investigated in order to determine whether some beneficial recovery results.

Testing is done in four-point flexure in an argon atmosphere furnace. The load is recorded continuously versus time. Deflection is measured with a probe system converted to an LVDT which is also continuously recorded versus time in order to be able to determine stress, strain and strain rate throughout the test.

Reduction of the bend test data to stress-strain curves has proved to be somewhat more difficult than expected. A technique has been previously developed for reducing a series of bend tests to stress-strain curves using the relations for outer fiber stress of[2]:

$$\sigma = \frac{2\,M}{bh^2}\,(2 + n_b + m_b) \qquad (1)$$

where $$n_b = \frac{\partial \ln M}{\partial \ln \varphi} \qquad (2)$$

$$m_b = \frac{\partial \ln M}{\partial \ln \dot{\varphi}} \qquad (3)$$

where M is the bending moment, φ the included angle of bending, $\dot{\varphi}$ the rate of bending and b and h the specimen width and height, respectively. The quantities n_b and m_b are determined empirically and generally depend somewhat upon φ and $\dot{\varphi}$. Several unexpected features have been revealed which complicate the analysis. Apparent yield phenomena resulting in discontinuities in some of the curves make application of these techniques more complicated. Further, markedly lower loads on reversal are observed. These are thought to indicate a reduced flow stress on reversal (Bauschinger effect); however, the possibility of a contribution from non-linearities in the stress distribution due to curvature and residual stresses are also being analyzed.

Since the analysis is not yet complete, the results presented here have been obtained using the approximate elastic equation in order to provide some comparative numbers; the usual equation has been used for the outer fiber stress:

$$\sigma = \frac{6\,M}{bh^2} \qquad (4)$$

Comparison with equation (1) indicates the order of error to be expected. In previous work m_b was shown to be approximately 0.6; this work shows that n_b may be as high as 0.4 so that the stress levels shown are approximately correct; some of the fine points, however, may not be in the correct perspective because of the dependence of n_b and m_b on φ and $\dot{\varphi}$.

Two composite stress-strain curves are presented in Figures 1 and 2 in which the absolute strain has been added. These two curves represent a difference in strain rate of nearly an order of magnitude. A similar curve for a test at an intermediate rate was presented in the first report.[1]

Several interesting features can be seen in all of these which are typical of additional similar tests. The initial flow stress has a high strain rate sensitivity as has been previously reported.[3] Significant rate sensitivity is still observed at higher stresses. These tests were done near the lower speed limit of this particular test machine where the speed control and uniformity is not as good as desired. Some of the waviness in the curves is caused by small changes in the cross-head velocity. Some of this may be aggrevated by non-uniform sliding along the knife edge although every attempt has been made to eliminate this or other frictional effects.

Since the curves have not yet been reduced to true stress-strain curves and because of the further uncertainty caused by the variable cross-head velocity, the fine points of the curves cannot be interpreted with certainty. Nevertheless, there are several features which are reproducible and significant enough to be worthy of comment at this time.

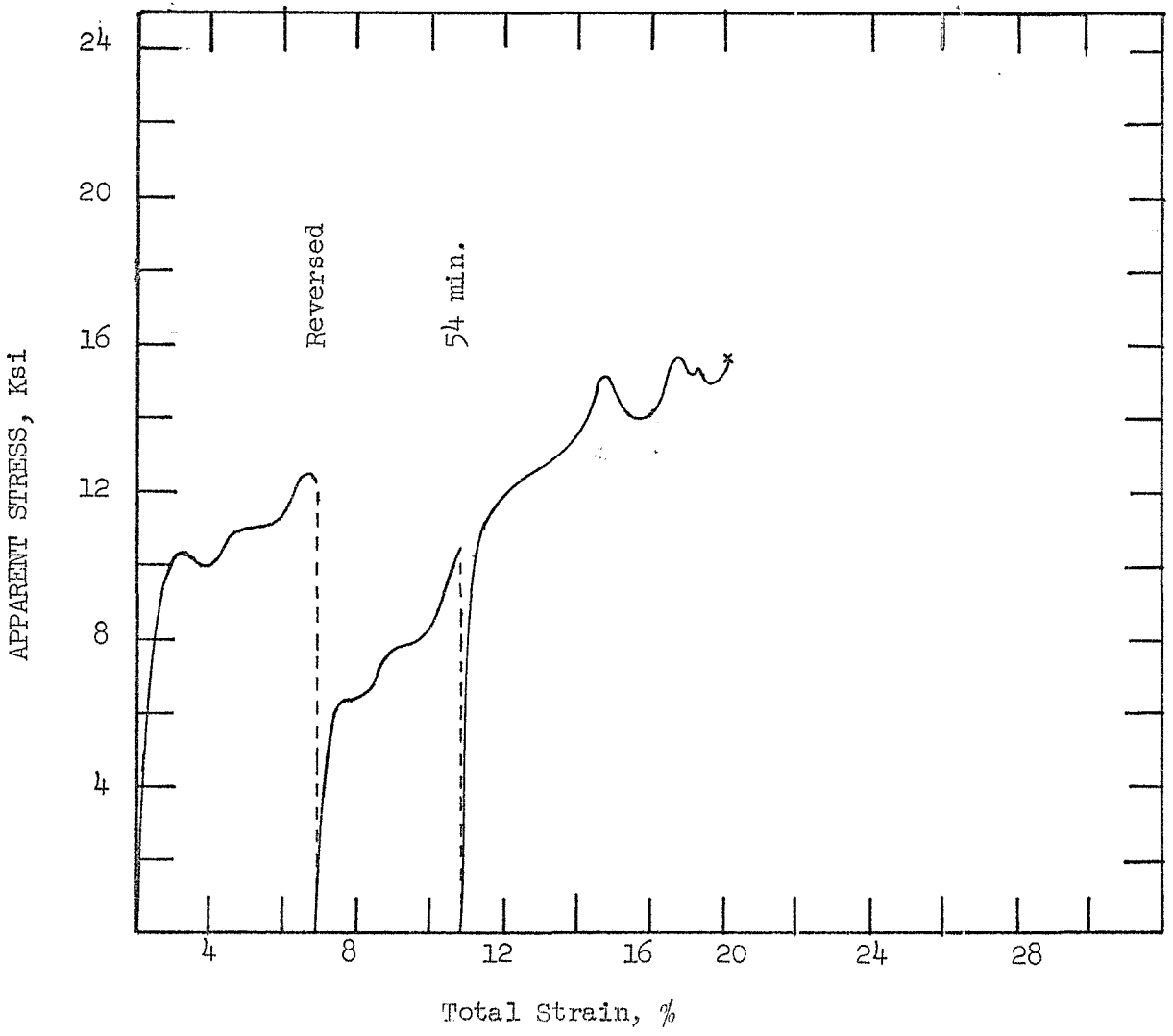
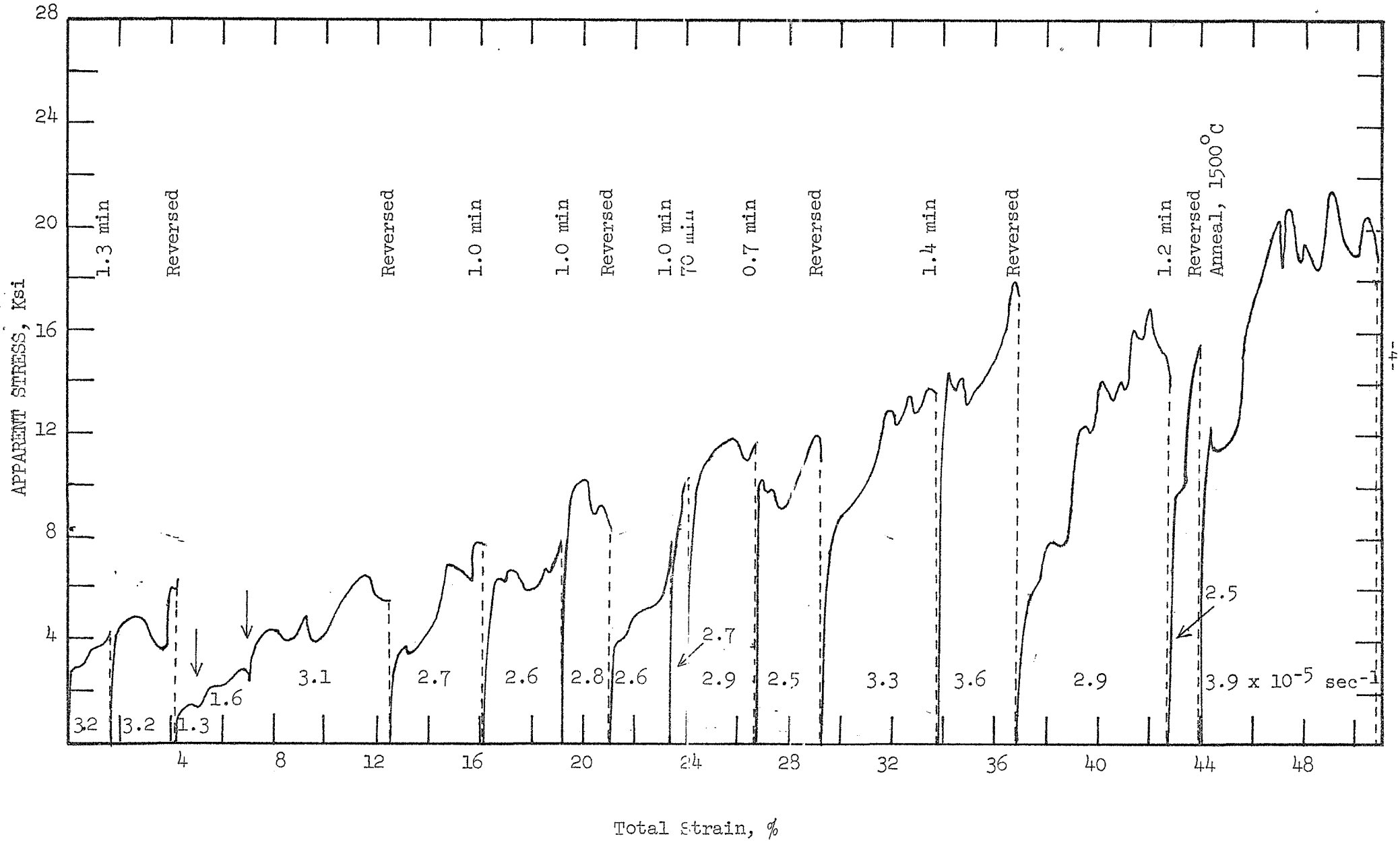


Figure 1. Apparent Stress vs. Strain Curve for Specimen FLUX-31 Tested at 1450°C and $\dot{\varepsilon} = 1.1 \times 10^{-4} sec^{-1}$

Figure 2. Apparent Stress vs. Strain Curve for Specimen FLUX-33 Tested at 1450°C. The average strain rate is shown for each part at the curve, including places where it was deliberately changed in cycle 2.



The curves all tend to have the same general shape and features. There is an initial region in which the stress rather quickly builds up to a particular level and then remains approximately constant for a while. Some of the curves suggest that there may be a strong yield phenomenon involved; however, the uncertainty introduced by small changes in rate preclude such a conclusion at this time. These changes may also be responsible for those curves in which this region is not completely flat.

After a small amount of strain (typically 0.5 to as much as 2%), a region of rapid strain hardening occurs which lasts for several percent strain. As the stress level increases the rate of hardening decreases somewhat although this effect appears to be influenced somewhat by the actual stress, strain and rate. The linear rate of strain hardening appears to be higher at higher strain rates; however, this does not hold indefinitely because of the high stress levels which are rapidly reached at the higher rates.

Unloading and reloading in the same direction results in rapid loading up to essentially the same stress level. There is generally a slight amount of recovery indicated by some non-linearity in the curves before reaching the previous stress level. A significant reduction in stress by recovery cannot be obtained even by holding at temperature for more than an hour before reloading. The new stress level is, however, sensitive to strain rate.

Reloading in the opposite direction results in a marked reduction in the flow stress. It is typically about half of the stress at the point of unloading. This is thought to be the result of a Bauschinger effect although the possibility of additional contributions from non-linear stress distributions are being analyzed. Not only is plastic flow initiated at a lower stress on reversal, but a short period of low strain hardening, similar to the initial yield period, is also seen.

With each successive cycle, the hardening effects become more pronounced. The region of constant yield stress becomes shorter and the Bauschinger effect becomes somewhat reduced. In addition, the linear rate of work hardening, taken from the steepest portion of the curve after reversal, increases with successive cycles.

Although the irregularities in the curves and the difficulties in the analysis obscure some of the finer points, the general trends described, all support the view that there is a strong process of strain hardening which becomes important after a couple of percent strain. This apparently is highly directional, but cyclic straining appears to eventually increase the hardening in both directions.

Specimen FLUX-33 was given a 1-hour anneal at 1500°C between the sixth and seventh cycle to determine whether recovery would result. Higher annealing temperatures are thought to be less desirable because of grain growth. Even this treatment did not result in any significant reduction in the flow stress. It did, however, seem to make the yield effect more pronounced.

Continued testing of these bars, eventually became impractical because strain hardening eventually caused much of the strain to occur out of the gage section as shown in Figure 3. This resulted in the strain distribution becoming so non-uniform that the nominal conditions for the bar were not satisfied well enough to continue testing.

The bars were always examined between cycles for evidence of crack formation. As previously reported, this material indicated an ability to withstand rather large cracks without failure after some strain was accumulated. The results to date suggest that cracking usually begins to occur when the apparent stress reaches about 15 Ksi. However, the more strain accumulated before this stress level is reached, the less likely and less serious the cracks will be. This suggests that the largest effect of strain rate on fracture is to allow more strain to accumulate before the flow stress builds up sufficiently high to cause cracking. This effect is enhanced by increased crack resistance resulting from accumulated strain.

Comparison of Figures 1 and 2 indicate further the effect of low strain rate and strain hardening in increasing the total strain before failure. At the high rate specimen FLUX-31 failed in the second cycle after about 16% total strain. Specimen FLUX-33, however, showed no cracking until after the fifth cycle (37% total strain) when a small crack appeared, shown in Figure 4, which did not propagate. Even after the sixth cycle the other side which was run at a slightly lower rate while in tension had no visible cracks. In the seventh cycle (approximately 50% total strain), apparent stresses over 20 Ksi were developed, but the crack only propagated a small amount further. Specimens tested at intermediate rates showed intermediate behavior.

III. MICROSTRUCTURAL EXAMINATION

Microscopic examination is being done on several of the specimens in order to provide mechanistic understanding and to assess the probable effects of forging on the material properties. Electron microscopy using a double replication technique has been used to date. The fine-grain size limits the usefulness of optical microscopy. Transmission microscopy through thin foils is planned for later in the program when an ion thinning device becomes available.

Extensive examination has been done on replicas from the as-tested surfaces on which thermal etching reveals many features and in which apparent deformation features can be seen, some of which are not fully understood at this time. The grain boundary regions are generally distorted indicating localized shear and probably some migration of the boundaries. Distorted and displaced triple grain junctions, as shown in Figure 5, are rather frequent, although these are more exaggerated than usual. The boundaries eventually become rather wide and indistinct. This supports the previously advanced view that grain boundary sliding (GBS) is a significant part of the deformation mechanism.

The tensile surfaces take much longer to develop deformation surface features than do the compression surfaces. The tensile surfaces appear only slightly different than untested, thermally etched samples for the first few cycles whereas the compression surfaces are extremely irregular after

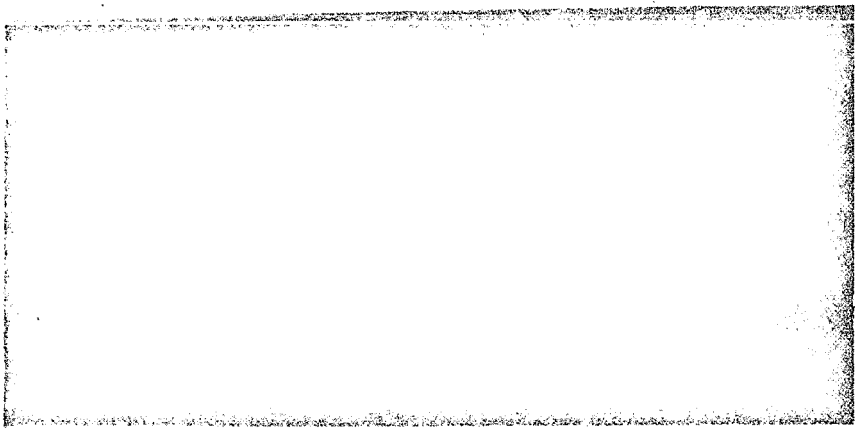


5172-5 5X

Figure 3. Specimen FLUX-33 After Testing Showing the Non-uniform Strain Caused by More Rapid Hardening of the Gage Section.

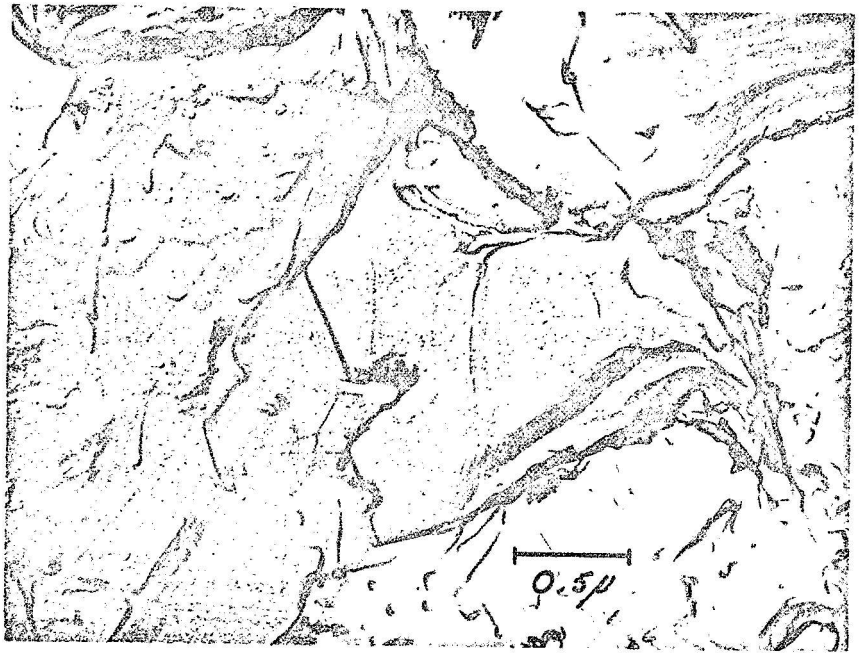


5172-2 (a) 20X

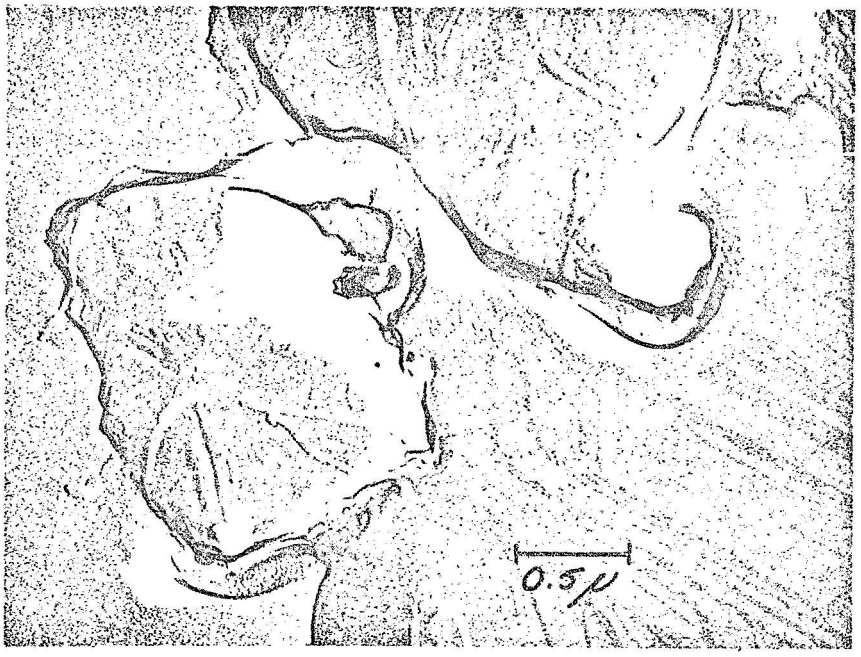


5172-6 (b) 20X

Figure 4. Crack in Specimen FLUX-33. This developed during the 5th cycle (a) and enlarged slightly after the 7th cycle (b).



69948 (a) 30,000X



691048 (b) 30,000X

Figure 5. Surface Replicas Showing Distorted Boundaries and Triple Grain Junctions. The top figure (a) is from the compressive surface of FLUX-32 after the third cycle and the lower is from the tensile surface of FLUX-33 after the sixth cycle.

the first cycle. After subsequent cycles the faces look more similar; however, the compressive surfaces always show more surface texture (thermal etching excepted) and more irregular boundaries. Examples of this from Specimen FLUX-33 can be seen in Figures 6 and 7. The causes of this are not fully understood at this time, however, they are being considered both in terms of the effect on deformation behavior particularly with respect to twinning and slip and in terms of the etching differences.

Several of these features suggest dislocation slip, particularly in the compressive surfaces. The sharp jogs in the grain boundary in Figure 5a are suggestive of slip band boundary intersections. In addition, steps on the surfaces are frequently seen which are thought to be different from the thermal etch faceting. Examples are shown in Figure 8. It is suggested these may result from the emergence of fine slip bands to the surface.

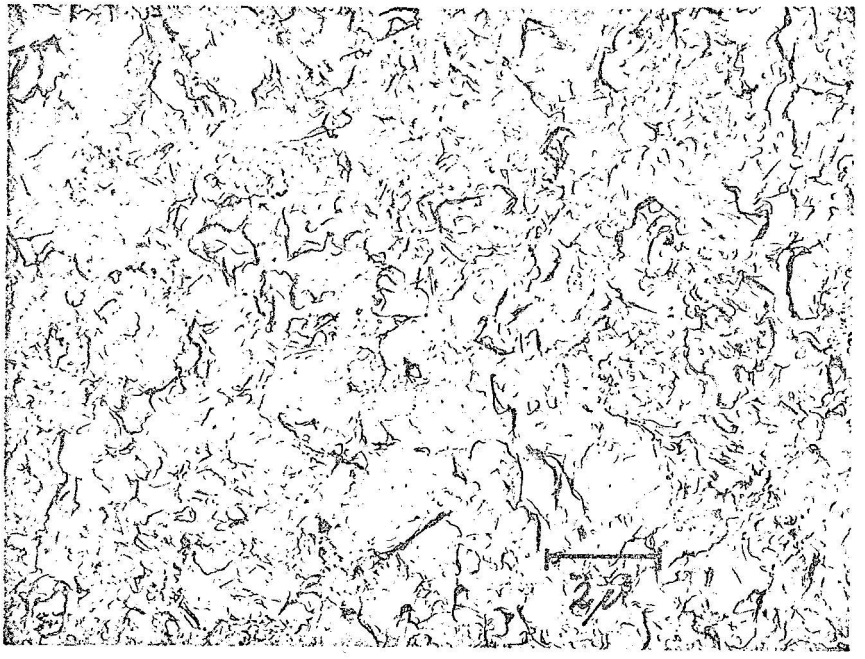
In order to ensure the generality of these results some polished and etched sections from the interior have also been examined. Irregular or curved boundaries with badly distorted triple junctions and wide or double boundaries are frequently found as shown in Figure 9. These essentially support the surface observations indicating extensive GBS. No positive evidence of dislocations has been found; however, no reliable procedures are known for dislocation decoration or etch pitting for alumina of this fine grain size. The competitive etching of the boundaries makes etching to resolve etch pits difficult. The cause of the fine spots in Figure 9a and the intragrain surface features in Figure 9b are not presently understood, but may be only etching artifacts.

Comparison of Figures 6 and 7 indicates that some grain growth occurs during the test; it is not certain at this time whether this is only a surface effect or not. Previous work has shown a strong grain size dependence on the flow stress in fine-grained alumina so that this may explain some of the increase in flow stress with successive cycles. The grain size was measured on one or the other of the surfaces after each cycle for two specimens and similar measurements were made for a control specimen which was put into the hot zone in various tests. The results are shown in Table I; they are uncorrected linear intercept values measured from photographs.

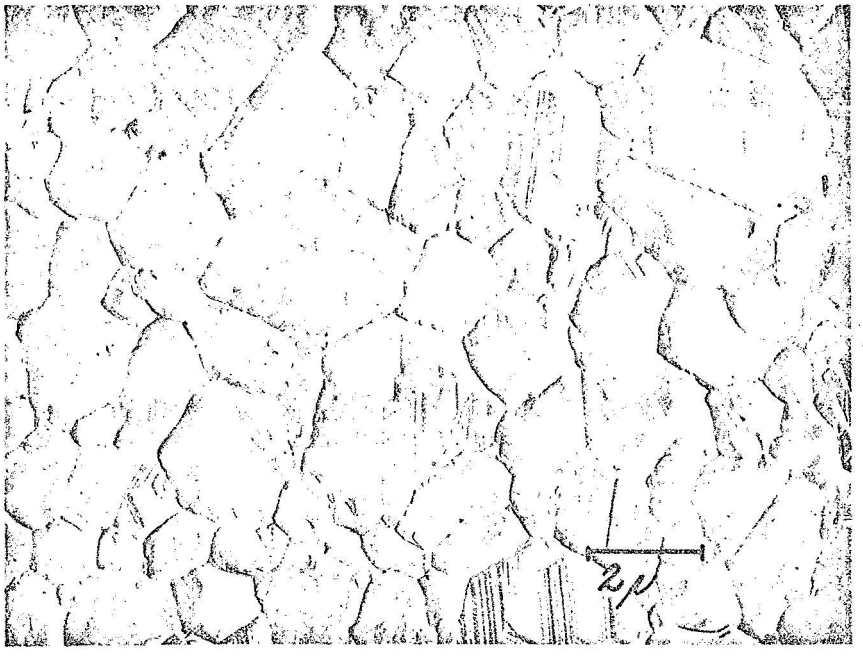
The lack of resolution of the boundaries in the compression surfaces prevented measurement of the grain size in a couple of instances. These data show that grain growth occurred and that it was enhanced by the concurrent deformation. Specimen FLUX-32 had a total strain range of 10% at a higher rate than FLUX-33 which had an average strain range of only 7.7%, so that the actual time per cycle was slightly shorter for FLUX-32. This indicates that the amount of grain growth per cycle is increased by a higher strain per cycle. Strain enhanced grain growth is perhaps not surprising if the deformation involves GBS accompanied by some concurrent boundary migration. This amount of grain growth may contribute to an apparent strain hardening and must be included in any mechanistic arguments.

IV. DISCUSSION

The mechanical test results indicate several surprising features which were not fully expected on the basis of previous work at low strains. The

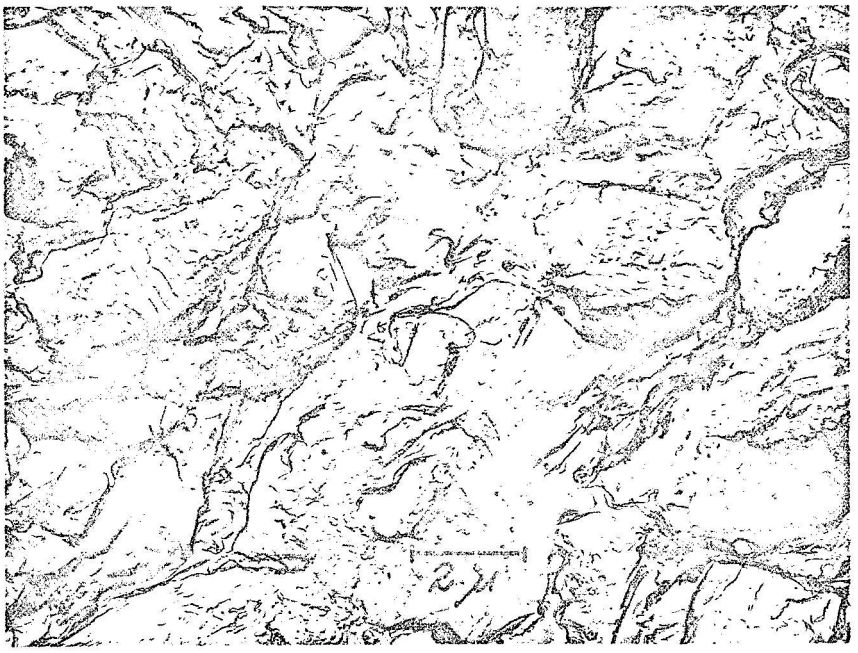


691009 (a) 7500X

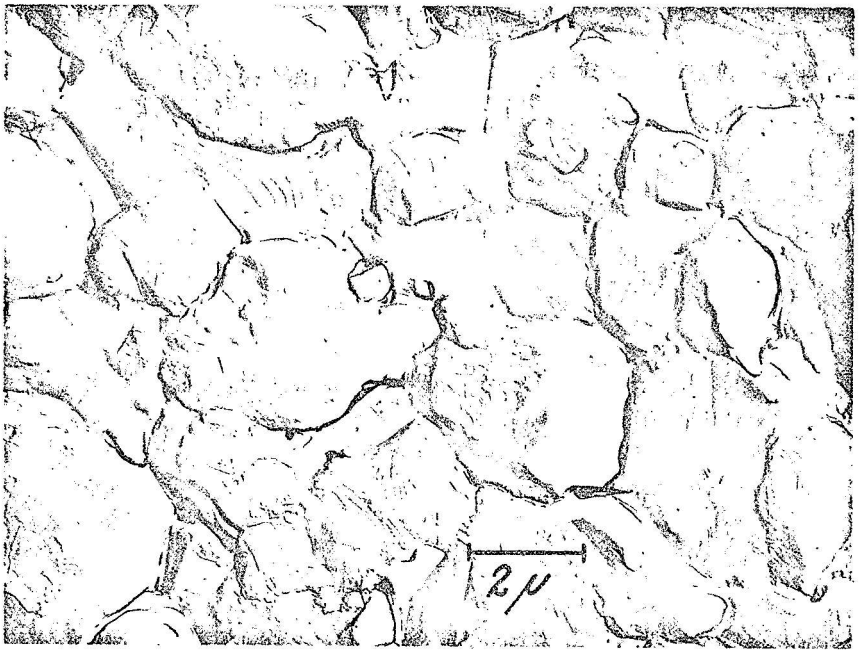


691015 (b) 7500X

Figure 6. Compressive and Tensile Surfaces after the 1st and 2nd Cycles, Respectively, for Specimen FLUX-33.

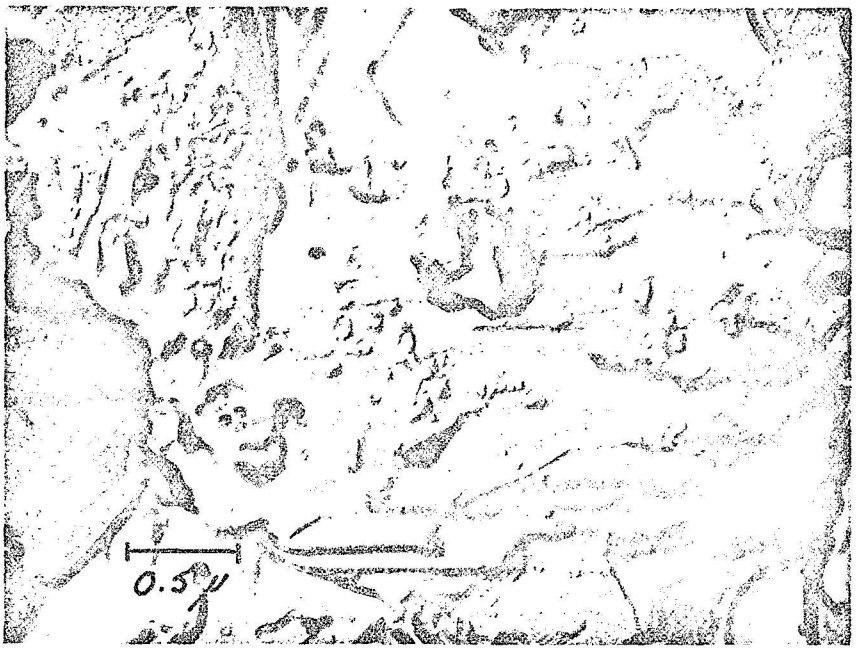


691049 (a) 7500X

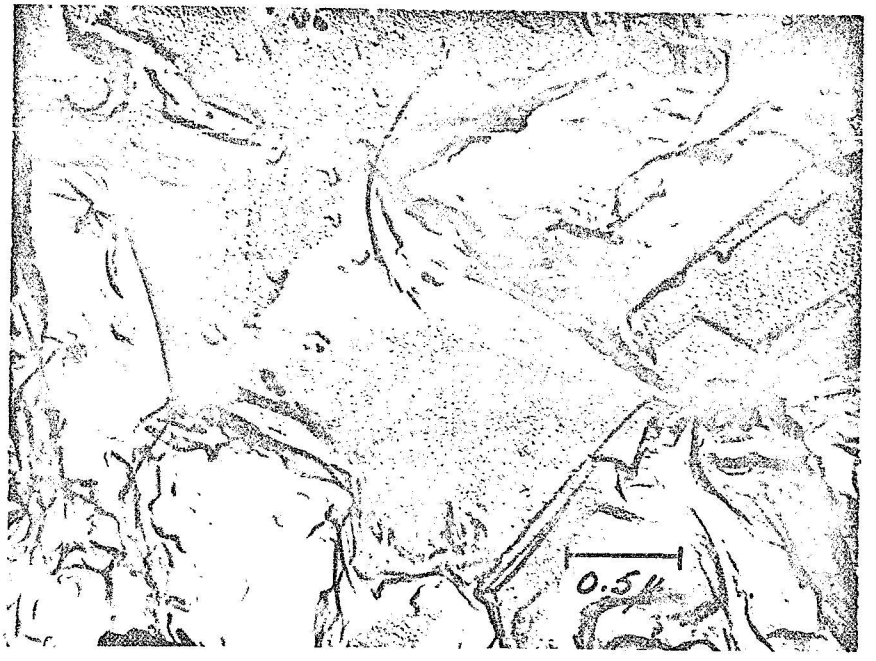


691043 (b) 7500X

Figure 7. Compressive and Tensile Surfaces after the 6th Cycle for Specimen FLUX-33.

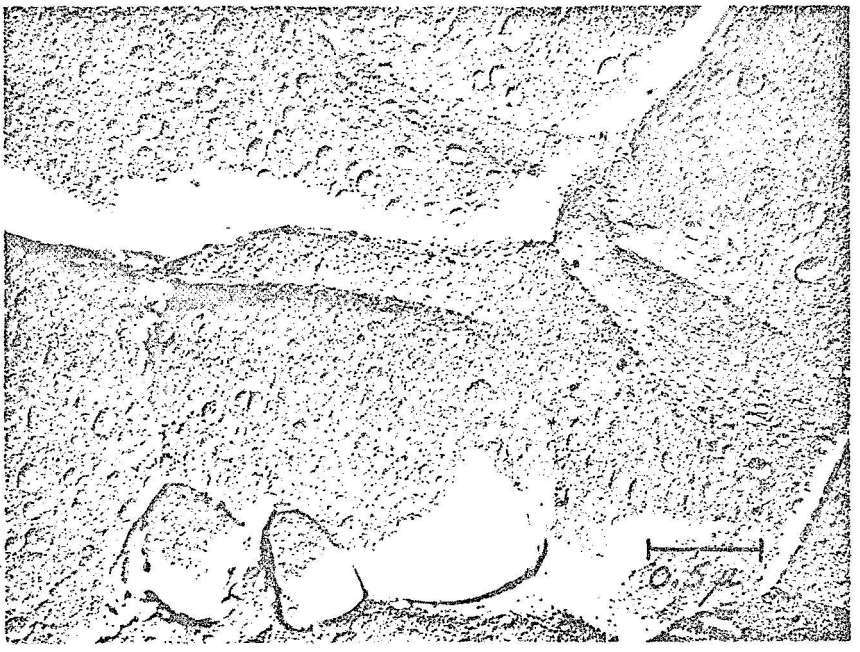


69946 (a) 30,000X

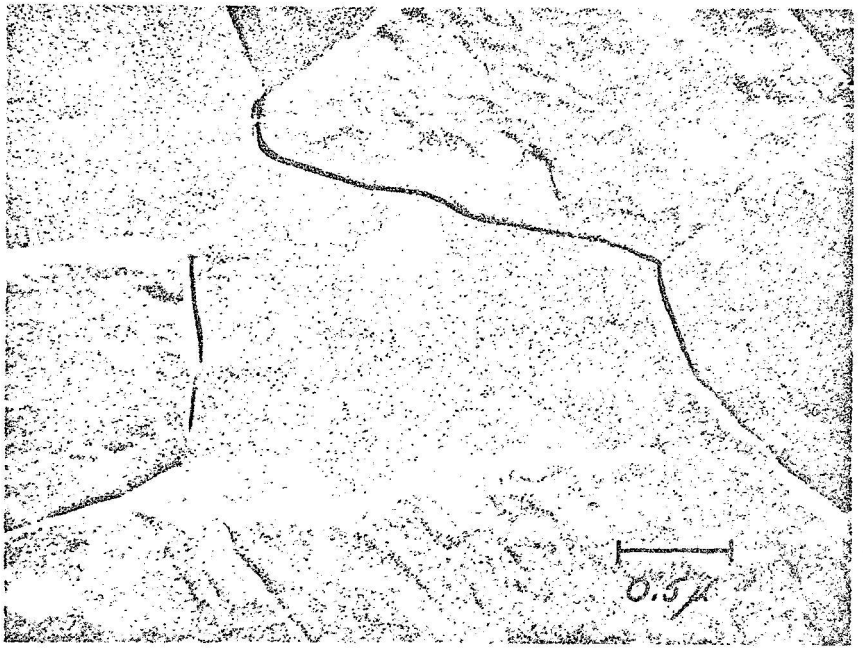


691053 (b) 30,000X

Figure 8. Fine Surface Steps Seen Primarily on Compresion Surfaces Which are Suggestive of Fine Slip Bands. The top figure is from the compression surface of FLUX-32 after the third cycle; the lower one is from the compressive surface of FLUX-33 after the sixth cycle.



70254 (a) 30,000X



70262 (b) 30,000X

Figure 9. Polished and Etched Cross-Sections from Specimen FLUX-30 Showing Distorted Boundaries and Triple Junctions.

TABLE I

GRAIN GROWTH IN SUCCESSIVE TEST CYCLES AT 1450°C

Cycle	FLUX-32	FLUX-33	FLUX Control
Initial	1.08 μ, A	-	-
1	1.70 μ, A	-	1.28 μ
2	1.47 μ, A	1.37 μ, A	1.37 μ
3	1.85 μ, A	1.65 μ, A	1.50 μ
4	2.24 μ, A	1.96 μ, A	1.75 μ*
5		2.09 μ, B	1.78 μ
6		1.96 μ, A	
Anneal 1500°C		1.96 μ, A	
7		2.24 μ, B	

* 1500°C Anneal, 1 hr.

The actual surface from which the measurement was taken is denoted by A or B.

apparent yield phenomena, the strong work hardening region and the Bauschinger effect all suggest that the GBS process involves additional slip and is not simply a viscous process in combination with diffusional creep. It has previously been suggested that GBS in alumina involved some dislocations at the boundaries.[3,1] This work is taken to support that suggestion.

The microstructural data provides unequivocal support for a mechanism involving GBS. It too, however, suggests that an additional contribution from crystallographic processes such as slip is important. The problem of concurrent grain growth further complicates interpretation of the data and will be considered more extensively. Further discussion of deformation mechanisms is held until the analysis of the flexural data is complete and some of the microstructural uncertainties are resolved.

The strong apparent stress dependence on fracture is somewhat surprising. It was initially expected that larger strains would lead to reduced fracture stresses as the result of intergranular separation. This type of information is extremely valuable in interpreting failure problems in forging and extending forgability. Similar understanding must be developed for uni-directional straining. Mechanistic understanding of this fracture behavior must be correlated with the deformation mechanisms.

V. FUTURE WORK

During the next quarter the analysis of the bend tests will be finished. An additional series of bend tests is planned in order to provide more reliable data on the grain size dependence of the plastic flow in fine-grained alumina. After the flexural tests are completed a series of torsion tests will be initiated to provide further, more accurate flow stress information at higher strains. Tensile testing is also planned to allow testing to failure at large strains in order to provide more information on fracture behavior.

The initial forgings are also planned for the next quarter. Initial efforts will be on a deep drawn hemisphere. Consideration is also being to closed die forging of a rib and web type of configuration.

VI. REFERENCES

1. R.M. Cannon and W.H. Rhodes, "Deformation Processes in Forging Ceramics," Progress Report 1, Contract NASW-1914 (19 June - 19 September, 1969).

2. A.H. Heuer and R.M. Cannon, "Plastic Deformation of Fine-Grained Aluminum Oxide," presented at Symposium in Mechanical Testing Procedures for Brittle Materials, IITRI, Chicag, Ill., March 28-30, 1967.

3. A.H. Heuer, R.M. Cannon and N.J. Tighe, "Plastic Deformation in Fine-Grain Ceramics," Ultrafine-Grain Ceramics, ed. J.J. Burke, N.L. Reed, V. Weiss, Syracuse Press, 1970.